CrystEngComm

COMMUNICATION

View Article Online
View Journal | View Issue

Cite this: *CrystEngComm*, 2022, **24**, 5405

Received 15th May 2022,
Accepted 6th July 2022

DOI: 10.1039/d2ce00665k

rsc.li/crystengcomm

Facile solvothermal synthesis of plate-like submicron $NaNbO_3$ particles†

Shingo Machida, *[a] Shoma Niwa,[a] Sho Usuki, [b] Kazuya Nakata, [c] Makoto Ogawa, [de] Atsuo Yasumori [a] and Ken-ichi Katsumata *[a]

Plate-like particles of orthorhombic $NaNbO_3$ were obtained *via* a solvothermal reaction using a methanol/ethanol mixed solvent, in contrast to the formation of cubic $NaNbO_3$ particles from methanol alone. Control of the submicron $NaNbO_3$ particle morphology was achieved by simply changing the solvent, suggesting the role of ethanol in suppressing the growth in one direction.

The discovery of the Honda–Fujishima effect, *i.e.*, the decomposition of water by titanium dioxide (TiO_2) photocatalysis, prompted researchers to investigate the fundamental properties and practical applications of photocatalysts.[1–4] Titanium oxide (TiO_2) has been widely studied because of its high activity, photo-induced hydrophilicity utilized for the self-cleaning effect, and low cost.[1–4] Additionally, TiO_2 is well-known as a white pigment[2,5–7] that requires submicron-sized particles to achieve its hiding power,[7,8] which is enhanced when the particle shape is platy.[9] One drawback of TiO_2 as a white pigment is its photocatalytic activity, which causes degradation of fabrics and resins.[1,2] The photo-induced hydrophilicity of sodium niobate ($NaNbO_3$) was first discovered by Katsumata and co-authors,[10,11] and $NaNbO_3$ shows potential as a photocatalyst, though with weaker activity than TiO_2,[10] and as a white pigment. The former case is promising for investigating the mechanisms of photo-induced hydrophilicity suppressed by photo-oxidation, while the latter case has high expectations for the particle shape and size of $NaNbO_3$, which possesses a perovskite-type (ABO_3) structure with an orthorhombic unit cell.[12] Well-defined cubic particles are thus typically obtained.[12–22] Submicron particles are prepared by solvothermal syntheses using synthesized niobium pentoxide (Nb_2O_5) and methanol as the raw materials.[16,17] In contrast, micron-sized and/or aggregated plate-like $NaNbO_3$ particles are prepared *via* hydrothermal syntheses[20–24] or topochemical ion exchange reactions of $Bi_{2.5}Na_{3.5}Nb_5O_{18}$, an Aurivillius phase layered perovskite, in molten sodium salts.[25–27] Submicron $NaNbO_3$ particles with a plate-like morphology are advantageous not only for photocatalytic activity through exposed surface design but also for higher hiding power in white pigment applications.

In this study, we devoted special attention to the facile preparation of plate-like submicron $NaNbO_3$ particles. The products were prepared by a modified version of the procedure reported in previous studies.[18,19] After dispersing 500 mg of Nb_2O_5 (obtained from Kojundo Chemical Laboratory Co., Ltd.) in 25 mL of methanol (MeOH)/ethanol (EtOH) mixed solvent (1 : 10 vol%), the dispersion was mixed with 5 mL of sodium hydroxide (NaOH) aqueous solution (10 mol L^{-1}). The obtained dispersion was placed in a Teflon vessel with a stainless jacket and then heated at 180 °C for 6, 24, or 48 h. After the reaction, the resultant solids were obtained by centrifugation, exhaustively washed with distilled water and methanol, and then dried at 80 °C for 1 h, to form the products denoted herein as $NaNbO_3$-(1Me+10Et)-6h, $NaNbO_3$-(1Me+10Et), and $NaNbO_3$-(1Me+10Et)-48h, respectively. For comparison, these procedures with a reaction time of 24 h were applied to cases using 25 mL of MeOH, EtOH, or MeOH/EtOH mixed solvent (1 : 4 vol%) instead of the MeOH/EtOH mixed solvent (1 : 10 vol%) to

[a] *Department of Material Science and Technology, Faculty of Advanced Engineering, Tokyo University of Science, 6-3-1 Niijuku, Katsushika-ku, Tokyo 125-8585, Japan. E-mail: shingo.machida@rs.tus.ac.jp, k.katsumata@rs.tus.ac.jp*
[b] *Graduate School of Bio-Application and Systems Engineering, Tokyo University of Agriculture and Technology, 2-24-16 Naka-cho, Koganei, Tokyo 184-0012, Japan*
[c] *Division of Sciences for Biological System, Institute of Agriculture, Tokyo University of Agriculture and Technology, 2-24-16 Naka-cho, Koganei, Tokyo 184-0012, Japan*
[d] *School of Energy Science and Engineering, Vidyasirimedhi Institute of Science and Technology, 555 Moo 1 Tumbol Payupnai, Amphoe Wangchan, Rayong 21210, Thailand*
[e] *Japan Advanced Institute of Science & Technology, 1-1 Asahidai, Nomi, Ishikawa 923-1292, Japan*

† Electronic supplementary information (ESI) available. See DOI: https://doi.org/10.1039/d2ce00665k

generate products denoted herein as $NaNbO_3$-Me, $NaNbO_3$-Et, and $NaNbO_3$-(1Me+4Et), respectively. In addition, the reactions for MeOH and MeOH/EtOH mixed solvent (1 : 10 vol%) were conducted by changing the amount of Nb_2O_5 from 500 mg to 5 g, to form the products denoted herein as $NaNbO_3$-Me-5g and $NaNbO_3$-(1Me+10Et)-5g, respectively. Moreover, the reactions for $NaNbO_3$-(1Me+10Et) were modified by decreasing the reaction temperature to 150 °C or the NaOH aqueous solution (5 mL) to 2 mol L^{-1}, to generate the products denoted herein as $NaNbO_3$-(1Me+10Et)-150°C and $NaNbO_3$-(1Me+10Et)-low-NaOH, respectively. The crystalline phases of the raw material and the products were characterized by X-ray diffraction (XRD) analyses (XRD-6100, Shimadzu). The particle shapes of the raw material and products were characterized by field-emission scanning electron microscopy (FE-SEM) (spra40, Zeiss). The photocatalytic properties of the products were briefly examined by performing decomposition of methylene blue (MB) using 50 mL of MB aqueous solution (1.0×10^{-5} mol L^{-1}) containing 50 mg of $NaNbO_3$-Me or $NaNbO_3$-(1Me +10Et) under 365 nm irradiation for 1 hour. Prior to these experiments, the dispersions were stirred for 2 h in the dark. The photocatalytic experiments were also performed using Degussa P25 standard for comparison purposes. The absorption spectra of $NaNbO_3$-Me and $NaNbO_3$-(1Me+10Et) were recorded using a JASCO v-670 spectrophotometer. Before these analyses, the samples were mixed with barium sulfate. The surface areas of $NaNbO_3$-Me and $NaNbO_3$-(1Me+10Et) were determined to be 4.8 and 6.0 m^2 g^{-1}, respectively, from the nitrogen adsorption isotherms measured at −196 °C (Belsorp MINI, MicrotracBEL) using the Brunauer–Emmett–Teller (BET) method.[28]

Fig. 1 shows XRD patterns for Nb_2O_5 and the products. All the patterns (Fig. 1b–d) show diffraction lines attributed to the orthorhombic phase of $NaNbO_3$,[13–19] along with the disappearance of reflections due to the orthorhombic phase of Nb_2O_5 (Fig. 1a).[13–19] Notably, the space group for the orthorhombic phase of $NaNbO_3$ is classified as *Pbcm*[12,13] or *Pbma*,[14,15] both are equivalent in different settings. For simplicity, we thus tentatively index the reflections observed in the XRD patterns of the products to those of *Pbcm*.[12] Fig. 2 presents the FE-SEM images of Nb_2O_5 and the products. The image of $NaNbO_3$-Me exhibits cube-like particles in the 50–500 nm range along with minute amounts of rod-like particles, while those of $NaNbO_3$-(1Me+10Et) and $NaNbO_3$-Et exhibit plate-like particles in the 100–800 nm range (Fig. 2b–d). Compared to the image of $NaNbO_3$-Et (Fig. 2d), that of $NaNbO_3$-(1Me+10Et) shows well-defined shapes and plate-like particles (Fig. 2c). Irregular-shaped particles in the 50–400 nm range observed in the image of Nb_2O_5 (Fig. 2a) are absent in all the product images. The absorption spectra of $NaNbO_3$-Me or $NaNbO_3$-(1Me+10Et) (Fig. S1†) exhibit broad signals at 320 nm, which is consistent with those reported previously.[16,17] Based on the MB decomposition fractions (Fig. 3), the photocatalytic activities of the present $NaNbO_3$-Me and $NaNbO_3$-(1Me+10Et) products were lower than that of P25. In previous studies,[10,11] $NaNbO_3$ films displayed a lower MB decomposition fraction than TiO_2 films. Also, the 34% MB decomposition fraction for $NaNbO_3$-(1Me+10Et) was approximately 1.25 times higher than that for $NaNbO_3$-Me (Fig. 3), in agreement with the BET surface areas for $NaNbO_3$-(1Me+10Et) (6.0 m^2 g^{-1}) and $NaNbO_3$-Me (4.8 m g^{-1}). Therefore, these results show that all the products are truly orthorhombic $NaNbO_3$ particles.

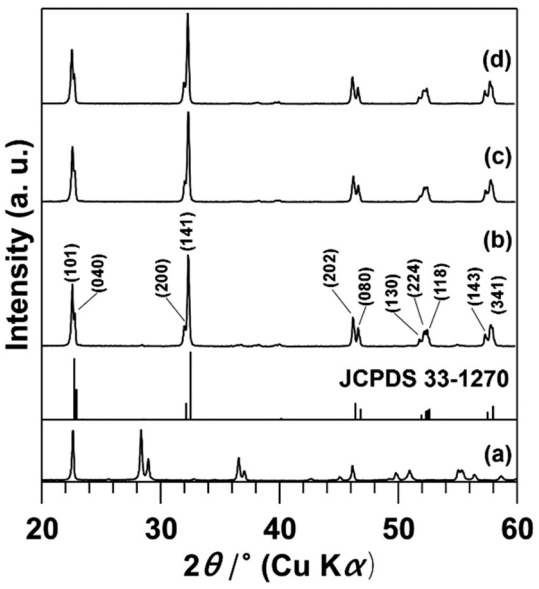

Fig. 1 XRD patterns for (a) Nb_2O_5, (b) $NaNbO_3$-Me, (c) $NaNbO_3$-(1Me +10Et), and (d) $NaNbO_3$-Et.

Notably, the plate-like particles form at a relatively early state of the reaction as suggested in the FE-SEM image of $NaNbO_3$-(1Me+10Et)-6h, which shows smaller and thinner plate-like particles than those of $NaNbO_3$-(1Me+10Et) (Fig. 2c and S2a†). The plate size reaches a maximum at about 24 h, since there are no major differences in the particle size range or shape observed between the FE-SEM images of $NaNbO_3$-(1Me+10Et) and $NaNbO_3$-(1Me+10Et)-48h (Fig. 2c and S2b†). When the MeOH/EtOH ratio in the mixed solvent was changed from 1 : 9 to 1 : 4 vol%, the thickness of the plate-like particles increased from 20–80 nm to 50–250 nm, as shown in the FE-SEM images of $NaNbO_3$-(1Me+10Et) and $NaNbO_3$-(1Me+4Et) (Fig. 2c and S2c†). Thus, the thickness of plate-like particles can be controlled by the reaction time or the MeOH/EtOH mixing ratio. In contrast, an increase in the amount of Nb_2O_5 as a raw material causes the formation of cube-like particles as exhibited in the FE-SEM image of $NaNbO_3$-(1Me+10Et)-5g, which is similar to $NaNbO_3$-Me-5g (Fig. S2d and e†). Cube-like particles also form when the reaction temperature or the NaOH concentration is decreased, based on the FE-SEM images of $NaNbO_3$-(1Me +10Et)-150°C and $NaNbO_3$-(1Me+10Et)-low-NaOH (Fig. S2f and g†). Based on these results, crystal growth in certain directions is suppressed for cubic $NaNbO_3$ particles under the reaction conditions that form plate-like particles. Feasible mechanisms are discussed below.

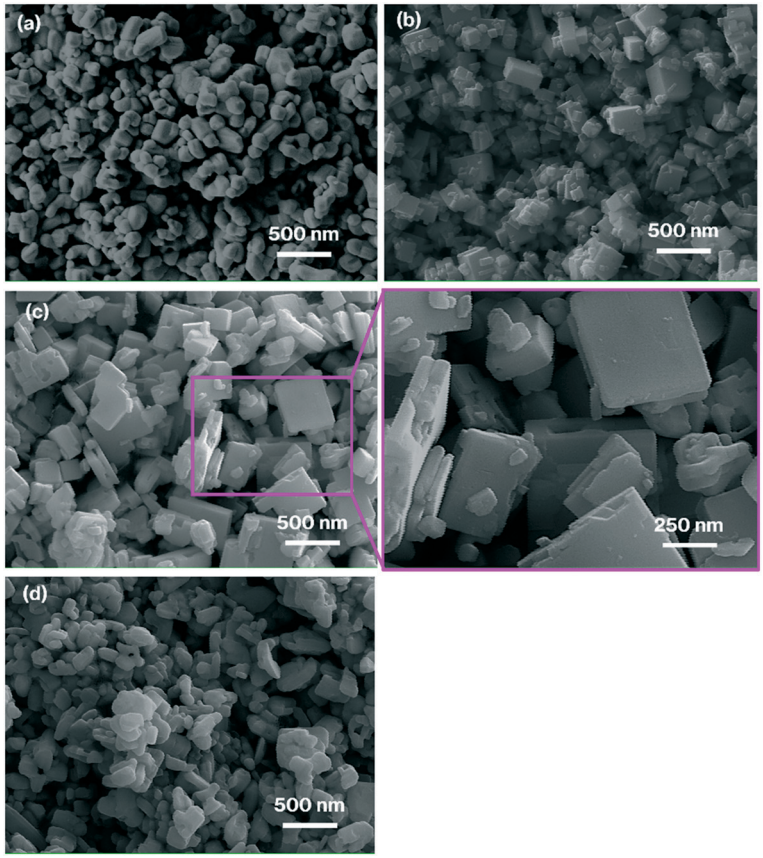

Fig. 2 FE-SEM images of (a) Nb_2O_5, (b) $NaNbO_3$-Me, (c) $NaNbO_3$-(1Me+10Et), and (d) $NaNbO_3$-Et.

It is well-known that hydrothermal reactions of the orthorhombic phase of Nb_2O_5 in the presence of a strong base generate cubic $NaNbO_3$ with the same phase, with sizes of 50 nm–20 μm,[15–22] while those in the 50–200 nm range are highly aggregated[22] and are prepared using relatively small amounts of Nb_2O_5 and dilute NaOH solution.[14] In addition, cubic particles of $NaNbO_3$ typically form *via* fibrous sodium niobate hydrate ($Na_2Nb_2O_6{\cdot}nH_2O$) as the intermediate.[16,17,20,22] In the literature, possible mechanisms for converting fiber- into cubic-particles have been presented,[16] but there is scant direct evidence for the process involved. Unfortunately, to the best of our knowledge, there have been no reports on the formation of fibrous sodium niobate hydrate ($Na_2Nb_2O_6{\cdot}nH_2O$) in solvothermal syntheses using alcohols. In addition, rod-like and orthorhombic $NaNbO_3$ particles have been synthesized hydrothermally, however, detailed formation mechanism is also absent.[22] A prior study found that methanol, with a lower dielectric constant than water, affected the raw material solubility for the solvothermal syntheses of $NaNbO_3$ as follows,[19] a large number of nuclei form, and the crystal growth is retarded when methanol is used instead of water, causing a decrease in the maximum sizes of cubic $NaNbO_3$ particles from 600 nm to 2 μm to 100–300 nm.[19] As mentioned above,[17] the particle size of Nb_2O_5 is a possible factor to determine its solubility in a strongly basic solvent. The size of the Nb_2O_5 particles used in the previous studies was 100–500 nm as judged from the FE-SEM images.[19] This size range is similar to that of the present Nb_2O_5 particles, although smaller particles are also present, as shown in the SEM image (Fig. 2a). Therefore, the present results for $NaNbO_3$-Me in the 50–500 nm range (Fig. 2b) are mostly consistent with previously reported values[18,20] and show that the size distribution of cubic

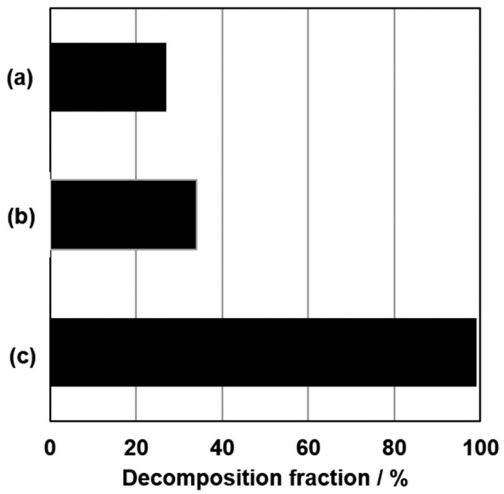

Fig. 3 MB decomposition fraction for (a) $NaNbO_3$-Me, (b) $NaNbO_3$-(1Me+10Et), and (c) P25.

$NaNbO_3$ particles is wider than the reported values.[17] In the previous reports on the hydrothermal synthesis of plate-like $NaNbO_3$ particles in the 200 nm to 1 μm range,[20–22] aggregated particles form at relatively short reaction times, whereas longer reaction times generate cubic $NaNbO_3$ particles. Plate-like particles likely form at an early stage of the hydrothermal synthesis, and the growth rate in the direction to convert plate-like particles into cubic particles seems to be rapid. Judging from the SEM images of the plate-like particles obtained by hydrothermal synthesis,[20–22] they are thinner than those in the present study using solvothermal synthesis (Fig. 2b and c). In the present study, plate-like orthorhombic $NaNbO_3$ particles form when ethanol is used as the solvent. The dielectric constant of ethanol is lower than that of methanol.[27] In addition, the dielectric constant of a mixture of methanol and ethanol decreases with an increasing ethanol content.[29] Based on the aforementioned discussion on the solvothermal synthesis of $NaNbO_3$, the rapid formation and preservation of plate-like particles, and the decrease in their thickness with an increasing ethanol content in the mixed solvent shown in the FE-SEM images (Fig. 2c and S2a–c†),[19] ethanol likely acted to retard the crystal growth more compared to methanol. The unit cell of orthorhombic $NaNbO_3$ is longer in one direction than in the other directions, *i.e.*, four NbO_6 octahedra bridged *via* the vertices are longer in one direction.[12,30,31] Based on the crystal structure of $NaNbO_3$ determined in a previous study,[12] the electron density in the longer direction for orthorhombic $NaNbO_3$ is lower than that in other directions.[12] Additionally, step- and kink-like structures[30] are present on the surfaces of the plate-like particles of $NaNbO_3$-(1Me+10Et) (Fig. 2c). Therefore, the crystal growth of $NaNbO_3$ in the ethanol and methanol mixture is likely to be suppressed in certain directions, causing the formation of plate-like particles. The plate-like particles in the present study are thus unlikely to grow into cubic particles, which is consistent with the formation of cube-like particles with increasing amount of raw material that could cause particle to grow in the thickness direction (Fig. 2c and S2d†). In addition, a decrease in the reaction temperature and base concentration may retard the growth of plate-like particles in the lateral direction, thus forming cube-like particles (Fig. 2c and S2f and g†). Such growth suppression in one direction could be utilized in further studies on the design and control of both the thickness and the lateral size of particles with a plate-like morphology.[32] In addition, compared to the ethanol and methanol mixture, a larger number of nuclei and a lower solubility of Nb_2O_5, which leads to less availability of the Nb source, may likely cause the formation of smaller and irregular plate-like particles when ethanol is used solely as the solvent. A decrease in the particle size of $NaNbO_3$ by ethanol addition is feasible judging from previous reports,[18,19,33] although the experimental conditions including the niobium sources in these previous studies are not identical. In addition, the particle size in other ABO_3 perovskites, such as potassium niobate ($KNbO_3$) and barium titanate, prepared by solvothermal synthesis increases by changing the solvent from methanol to ethanol.[34,35] Thus, reports on the solvothermal syntheses of other ABO_3 perovskites including those using a mixture of methanol and ethanol[36,37] are not very helpful for clarifying the growth mechanisms involved in the present study. Interestingly, although in previous studies the particle morphology of $KNbO_3$ changed very little when using a mixed solvent,[34] in the present study, the $NaNbO_3$ particle shape was successfully changed from cubic to plate-like. Note that there are non-linear relationships between specific solvent parameters for methanol–ethanol mixtures and the methanol or ethanol content.[29] Therefore, the effects of methanol–ethanol mixed solvents on the morphology of $NaNbO_3$ particles are worth further investigating, and it is thought that fibrous sodium niobate hydrate ($Na_2Nb_2O_6{\cdot}nH_2O$) could play a role. Nevertheless, the cubic- and plate-like $NaNbO_3$ particles identified in the present study, exhibiting photo-inducted properties, may find practical applications.[10,11,38–40] The photocatalytic activity of plate-like $NaNbO_3$ could be especially dependent on its morphology because there is a relationship between the MB decomposition fraction and the BET surface area for cubic- and plate-like $NaNbO_3$, despite the lower water dispersibility of plate-like $NaNbO_3$ (Fig. S3†). Such studies are ongoing in our laboratory, and the results will be reported in due course.

In summary, we have demonstrated the formation of platy submicron-sized $NaNbO_3$ particles *via* solvothermal synthesis using a methanol/ethanol mixed solvent (1 : 10 vol%). The results of the present study could potentially lead to a method for producing a wide range of perovskite compounds[41] with a plate-like morphologies.

Author contributions

Shingo Machida: conceptualization, investigation, data curation, writing – original draft, preparation, and project administration; Shoma Niwa: data curation; Sho Usuki: writing – review and editing; Kazuya Nakata: writing – review and editing; Makoto Ogawa: writing – review and editing; Atsuo Yasumori: project administration; Ken-ichi Katsumata: conceptualization, writing – review and editing, and supervision.

Conflicts of interest

The authors declare no conflicts of interest.

Acknowledgements

This research was supported by a Grant-in-Aid from the moon-shot project (JPNP18016) "Development of photo-switching ocean-degradable plastics with edibility" of New Energy and Industrial Technology Development Organization (NEDO), Japan.

References

1 A. Fujishima, T. N. Rao and D. A. Tryk, *J. Photochem. Photobiol., C*, 2000, **1**, 1–21.
2 K. Hashimoto, H. Irie and A. Fujishima, *Jpn. J. Appl. Phys.*, 2005, **44**, 8269–8285.
3 K. Nakata and A. Fujishima, *J. Photochem. Photobiol., C*, 2012, **13**, 169–189.
4 W. Lei, N. Suzuki, C. Terashima and A. Fujishima, *Front. Energy*, 2021, **15**, 577–595.
5 C. F. Goodeve, *Trans. Faraday Soc.*, 1937, **33**, 340–347.
6 S. Bourtillier, S. Fourmentin and B. Laperche, *Environ. Chem. Lett.*, 2022, **20**(1033), 1017–1033.
7 J. H. Braun, A. Baidins and R. E. Marganski, *Prog. Org. Coat.*, 1992, **20**, 105–138.
8 G. K. van der Wel and O. C. G. Adan, *Prog. Org. Coat.*, 1999, **37**, 1–44.
9 M. J. A. Ruszala, N. A. Rowson, L. M. Grover and R. A. Choudhery, *Int. J. Chem. Eng. Appl.*, 2015, **6**, 331–340.
10 K. Katsumata, C. E. J. Cordonier, T. Shichi and A. Fujishima, *J. Am. Chem. Soc.*, 2009, **131**, 3856–3857.
11 K. Katsumata, C. E. J. Cordonier, T. Shichi and A. Fujishima, *Mater. Sci. Eng., B*, 2010, **172**, 267–270.
12 A. M. Hamilton, S. O'Donnell, B. Zoellner, I. Sullivan and P. A. Maggard, *J. Am. Ceram. Soc.*, 2020, **103**, 454–464.
13 H. Ge, Y. Hou, C. Xia, M. Zhu, H. Wang and H. Yan, *J. Am. Ceram. Soc.*, 2011, **94**, 4329–4334.
14 B. Zou, T. Wang, S. Li, R. Kang, G. Li, S. A. El-Khodary, D. H. L. Ng, X. Liu, J. Qiu, Y. Zhao, J. Lian and L. Huang, *J. Energy Chem.*, 2021, **57**, 109–117.
15 S. Ji, H. Liu, Y. Sang, W. Liu, G. Yu and Y. Leng, *CrystEngComm*, 2014, **16**, 7598–7604.
16 Q. Liu, L. Zhang, Y. Chai and W.-L. Dai, *J. Phys. Chem. C*, 2017, **121**, 25898–25907.
17 H. Zhu, Z. Zheng, X. Gao, Y. Huang, Z. Yan, J. Zou, H. Yin, S. H. Kable, J. Zhao, Y. Xi, W. N. Martens and R. L. Frost, *J. Am. Chem. Soc.*, 2006, **128**, 2373–2384.
18 K. Nakashima, Y. Toshima, Y. Kobayashi and M. Kakihana, *J. Asian Ceram. Soc.*, 2019, **7**, 36–41.
19 K. Nakashima, Y. Toshima, Y. Kobayashi, Y. Ishikawa and M. Kakihana, *J. Asian Ceram. Soc.*, 2019, **7**, 544–550.
20 T. Y. Ke, H. A. Chen, H. S. Sheu, J.-W. Yeh, H.-N. Lin, C.-Y. Lee and H. T. Chiu, *J. Phys. Chem. C*, 2008, **112**, 8827–8831.
21 H. Song and W. Ma, *Ceram. Int.*, 2011, **37**, 877–882.
22 G. F. Teixeira, E. Silva Junior, A. Z. Simões, E. Longo and M. A. Zaghete, *CrystEngComm*, 2017, **19**, 4378–4392.
23 Y. Lu, T. Karaki and T. Fujii, *J. Am. Ceram. Soc.*, 2015, **98**, 1668–1672.
24 L. Jiang, Y. Zhang, Y. Qiu and Z. Yi, *RSC Adv.*, 2014, **4**, 3165–3170.
25 Y. Yan, D. Liu, W. Zhao and H. Zhou, *J. Am. Ceram. Soc.*, 2007, **90**, 2399–2403.
26 X. Li, G. Li, S. Wu, X. Chen and W. Zhang, *J. Phys. Chem. Solids*, 2014, **75**, 491–494.
27 Z. Pan, B. Liu, J. Zhai, L. Yao, K. Yang and B. Shen, *Nano Energy*, 2017, **40**, 587–595.
28 S. Brunauner, P. H. Emmett and E. Teller, *J. Am. Chem. Soc.*, 1938, **407**, 309–319.
29 B. G. Lone, P. B. Undre, S. S. Patil, P. W. Khirade and S. C. Mehrotara, *J. Mol. Liq.*, 2008, **141**, 47.
30 M. Mohsen-Nia, H. Amiri and B. Jazi, *J. Solution Chem.*, 2010, **39**, 701–708.
31 P. G. Vekilov, *Cryst. Growth Des.*, 2007, **7**, 2796–2810.
32 S. Machida, T. Yoshida, R. Hashimoto and M. Ogawa, *J. Colloid Interface Sci.*, 2014, **420**, 66–69.
33 K. Oshima, K. Nakashima, S. Ueno and S. Wada, *Trans. Mater. Res. Soc. Jpn.*, 2015, **40**, 413–416.
34 K. Nakashima, S. Ueno and S. Wada, *J. Ceram. Soc. Jpn.*, 2014, **122**, 547–551.
35 K. Nakashima, K. Onagi, Y. Kobayashi, T. Ishigaki, Y. Ishikawa, Y. Yoneda, S. Yin, M. Kakihana and T. Sekino, *ASC Omega*, 2020, **6**, 9410.
36 Y. Yoneda, R. Kunisada, T. Chikata, S. Ueno, I. Fujii, H. Nagata, K. Ohara and S. Wada, *Jpn. J. Appl. Phys.*, 2019, **58**, SLLA03.
37 Y. Yoneda, R.-I. Kunisada, T. Chikada, S. Ueno, K. Ohara and S. Wada, *Trans. Mater. Res. Soc. Jpn.*, 2018, **43**, 93–96.
38 K. Matsui, M. Karasaki, M. Segawa, S. Y. Hwang, T. Tanaka, C. Ogino and A. Kondo, *Med. Chem. Commun.*, 2010, **1**, 209–211.
39 R. Nakano, M. Hara, H. Ishiguro, Y. Yao, T. Ochiai, K. Nakata, T. Murakami, J. Kajioka, K. Sunada, K. Hashimoto, A. Fujishima and Y. Kubota, *Catalysts*, 2013, **3**, 310–323.
40 S. F. Silva, F. A. Silva, A. P. Martins de Souza, T. S. Rodrigues and R. R. Teixeira, *J. Mater. Sci.*, 2022, **57**, 1669–1688.
41 K. Huang, L. Yuan and S. Feng, *Inorg. Chem. Front.*, 2015, **2**, 965–981.